Unravelling the collagen network of the arterial wall

Beenakker, J.W.M.

5 Mechanical properties of the aorta studied by enzymatic treatments

This chapter is currently in press as:
Mechanical properties of the extra cellular matrix of the aorta studied by enzymatic treatments
J. W. M. Beenakker, B. A. Ashcroft, J. H. N. Lindeman and T. H. Oosterkamp
Biophysics Journal, 2012

5.1 Abstract

The micro-architecture of different components of the extra cellular matrix is crucial to the understanding of the properties of a tissue. In the study presented here, we use a top-down approach to understand how the interplay between different fibers determines the mechanical properties of real tissues. By selectively removing different elements of the arterial wall, we are able to measure the contribution of the different constituents of the extra cellular matrix (ECM) to mechanical properties of the whole tissue. The change in the network structure is being imaged using two-photon microscopy. The Atomic Force Microscope is used to measure the change in mechanical properties by performing nano-indentation experiments.

We show that although the removal of a key element of the ECM reduced the local stiffness by up to 50 times, the remaining tissue still formed a coherent network. We also show how this method can be extended to study the effects of cells on real tissues. This new way of studying the ECM will not only help physicists gain a better understanding of biopolymers, it will be a valuable tool for biomedical researchers studying processes such as wound healing and cervix ripening.

5.2 Introduction

In addition to the different fibers and other components making up a tissue, the micro-architecture of the different components is crucial to the mechanical properties of a tissue. In recent years, different in vitro studies on reconstituted components of the extra cellular matrix (ECM) have shed a light on the physical principles that determine the mechanical properties of tissues. In such a bottom-up approach, one or two different ECM-components are combined to make a gel and reveal a rich interplay between fibers, linkers and cells.[1–4]

In the study presented here, we use a top-down approach to understand how the interplay between different components determines the mechanical properties of real tissues. By selectively removing different elements of the arterial wall, e.g. removing the collagen by collagenase, we were able to measure the contribution of the different constituents of the ECM to the mechanical properties of the tissue as a whole. Similar proteolytic treatments on the arterial wall have previously been used to study the spatial organisation of the fibers within the tissue using immunofluorescence[5] and scanning electron microscopy.[6] Despite the difficulties posed by the complexity of real tissues, this method allows the microarchitecture present in real tissues to be studied. Ultimately, this method

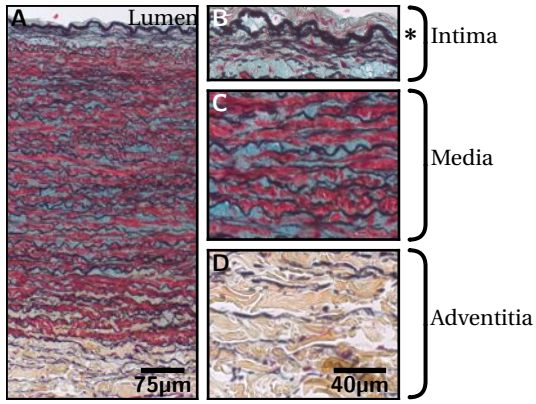

Figure 5.1:
Microscopic overview of the anatomy of the abdominal aortic wall using Movat pentachrome staining.
The aortic wall (A) is composed of multiple layers consisting of different builds. The intima (B) is the thin inner layer of the vessel wall, containing endothelial cells which are in contact with the lumen and is separated from the media (C) by the internal elastic lamina (∗). The tunica adventitia (D) contains mainly collagen (brown), while the tunica media also consists of elastin (dark blue/black) and smooth muscle cells (red). Proteoglycans (light blue) are present in both layers, but predominantly in the media.
(A) was taken at 100× magnification, (B–D) were taken at 400× magnification.

could be extended to study the effects of cells on the extra cellular matrix, e.g. by studying the effects of the contents of neutrophils on the extra cellular matrix. The change in the network structure is being imaged using two photon microscopy. Previous studies have used enzymatic digestions to differentiate the contributions of the different constituents of the ECM to the mechanical response of the whole tissue.[7–11] In this study, the Atomic Force Microscope (AFM) is used to measure the change in mechanical properties on the sub-micrometer scale by performing nano-indentation experiments.

5.3 Materials and Methods

All experiments have been performed on porcine aorta to minimize the biological variation between samples. Whole porcine aortas were collected within 18 hours after slaughter sliced in 15mm pieces and snap frozen in liquid pentane. The tissue was cryosliced to 50µm and stored at -80°C until used.

The aortic wall is composed of multiple layers consisting of different builds, as is shown in fig. 5.1. By studying the tunica adventitia, the collagen rich outer layer of the aorta, and the neighboring tunica media, which is rich in elastin and

Sample	Concentration	Temperature
Control/PBS	-	25 °C / 37 °C
Elastase (Worthington)	5.5 u/ml	25 °C
Collagenase (Worthington, type CLSPA)	200 u/ml	37 °C
Chodroitionas ABC (Sigma) + Hyalunoidase (Sigma)	1000 u/ml 0.04 u/ml	37 °C
Neutrophils	10 times diluted	37 °C

Table 5.1:
Concentrations of enzymes used for the various proteolytic treatments.
PBS was used as a buffer for al experiments except for the Chondroitinase ABC + Hyaluronidase, in which a 50 mM Tris (Sigma), 10 mM sodium (Sigma) acetate buffer was used for the incubation and all the sample preparation steps. Incubation took place in the presence of penicillin (50 units/ml, Sigma) + streptomycin (50 µg/ml, Sigma) to prevent the growth of bacteria. Elastase and collagenase are from Worthington Biochemical Corporation, Lakewood, NJ.

also contains some collagen fibers, we can examine the proteolytic effects on two different networks within one sample.

After thawing, the samples were put in PBS (137 mM NaCl, 2.7 mM KCl, 8 mM Na2PO4, 1.8 mM KH2PO4, pH 7.4, all from Sigma-Aldrich, Zwijndrecht, The Netherlands) for approximately 5 minutes to reconstitute. After removal of the PBS, the samples where covered with PBS with penicillin-streptomycin (50 units/ml) and the enzymes in a stove overnight at 37 °C, except for the elastin digestion which was performed overnight at 25 °C. The concentrations of the enzymes, listed in table 5.1, are chosen such that the specific components are removed, but the rest of the tissue remains intact.[9] The contents of neutrophils, activated by 100 nM formyl-Met-Leu-Phe (Sigma), were prepared as described in ref. [12]. After the proteolytic treatment, the buffer with enzymes is changed to PBS and the sample is used either for two-photon imaging or AFM nano-indentation.

Second-harmonic generation (SHG) was used to image the organization of the collagen and the elastin fibers.[13] To detect collagen we used filter settings to be sensitive for frequency doubling, while to detect elastin we relied on its autofluorescence. The two-photon microscopy was performed on a Zeiss 710 NLO (Jena, Germany) upright confocal microscope equipped with a Spectra-Physics Deep See MP laser (Spectra-Physics, Inc., Mountain View, CA). The images were obtained with an excitation wavelength of 800 nm and emitted light with a wavelength between 371 nm–425 nm was detected for the collagen signal and between 471 nm–532 nm for elastin. Confocal stacks were processed for maximum intensity projections with the Zeiss ZEN2009 software.

The AFM nano-indentation experiments are performed as described in chapter 3. In short, measurements were done using a Molecular Imaging Picoscan AFM (Agilent Technologies, Palo Alto, CA) controlled with a custom scripting program

written in LabVIEW (National Instruments, Austin, TX) and Visual Basic 6 (Microsoft, Redmond, WA). The nano-indentation was performed with a 0.58 N/m cantilever (NP type (Veeco Metrology, Santa Barbara, CA)) with a sharp tip and was recorded with a National Instruments card at 100 kS/s. MATLAB (The MathWorks, Natick, MA) was used to calculate the Young's modulus for each indentation using the FIEL method of Hassan et al.[14] This method calculates the work needed for a certain deformation by integrating the force-distance curve. This measure for the stiffness is compared to a modeled curve, calculated using the Hertz model,[15] that would be expected for a conical indenter. The spring constant, necessary to relate the cantilever deflection with the applied force, is calibrated with the thermal noise method.[16]

The assumption of the Hertz model of an isotropic, smooth substrate with a Young's modulus independent of the applied force, is not met. Biological tissues tend to stiffen when they are deformed,[3, 4] and the many different types of fibers make the sample far from isotropic. However, by keeping the loading rate approximately constant amongst different experiments and using the same force-setpoint, 20 nN, the calculated values for the stiffness can still be used as a measure of the response of the tissue upon indentation. This "effective Young's modulus" will reflect the local mechanical properties of the tissue under the set experimental conditions and can be used to compare indentations on different types of tissue.

By performing the indentations on a regular grid, a stiffness map of the tissue, with a corresponding stiffness distribution, is made. All AFM measurements are performed in buffer at 37 °C (control, collagenase, chondroitinase + hyaluronidase, neutrophils) or 25 °C (control, elastase). For every case at least 2000 indentations on different locations have been performed.

Samples for Scanning Electron Microscopy (SEM) imaging have been prepared and incubated with enzymes with the same method as for the AFM measurements. After overnight incubation with the enzymes, the samples were put overnight in PBS with 2% glutaraldehyde (Sigma) at 4 °C. Afterwards, the samples where critical point dried and coated with a thin layer of gold-palladium (maximal 5 nm thick) and stored at room temperature until use. A field emission SEM (JEOL JSM-6700F) was used at 5.0 kV.

5.4 Results and Discussion

Figure 5.2 shows a stiffness map measured on the tunica media of a sample without any enzymes added. Each pixel of the stiffness map represents the stiffness calculated from a single indentation curve, with light colors indicating

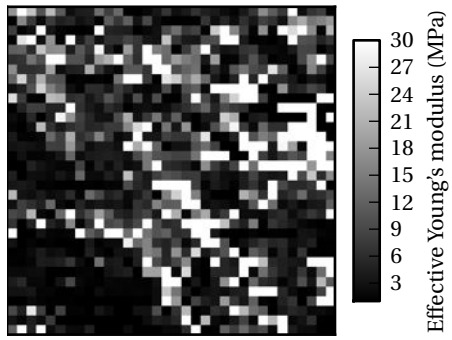

Figure 5.2:
Stiffness map measured on the tunica media of a sample without any enzymes added (113µm × 113µm, 34 × 34points). Stiffer pixels tend to be grouped in elongated patches which have an orientation that coincides with the fibers that are visible in the optical microscope integrated with the AFM.

large stiffness. The stiffness map shows that stiffer pixels tend to be grouped in elongated patches, which have an orientation that coincides with the fibers that are visible in the optical microscope integrated with the AFM. We combine multiple stiffness maps for every sample treatment into a single histogram, which reflects the distribution of stiffnesses within a sample. These histograms of the media and the adventitia are plotted in fig. 5.3, and show a clear change in effective Young's modulus for certain proteolytic treatments.

Figure 5.4 shows the two-photon images of the adventitia and media for the different proteolytic treatments we have performed. The two-photon images of the control show the difference in network structure between the media and adventitia. The adventitia consists of a densely woven network of collagen fibers, while the media consists mainly of parallel elastin fibers. The swelling stress of the proteoglycans, present in both layers of the arterial wall, puts the network, composed by the collagen and the elastin fibers, under tension.[17, 18] The small deformations made by the AFM tip mainly probe the tension on this combined network instead of the mechanical properties of the isolated fibers. The inhomogeneous distribution of proteoglycans across the vessel wall, showing a higher concentration in the media than in the adventitia,[19, 20] could give rise to the measured stiffer response in the media compared to the adventitia.[21, 22]

Digestion by elastase reveals the underlying collagen structure in the media and reduces the stiffness of the remaining tissue of the media, as was expected since elastin is one of its main components. The network structure and mechanics of the adventitia however remain unaltered by the elastin removal. Since the removal of elastin needed an incubation temperature of 25 °C, a control

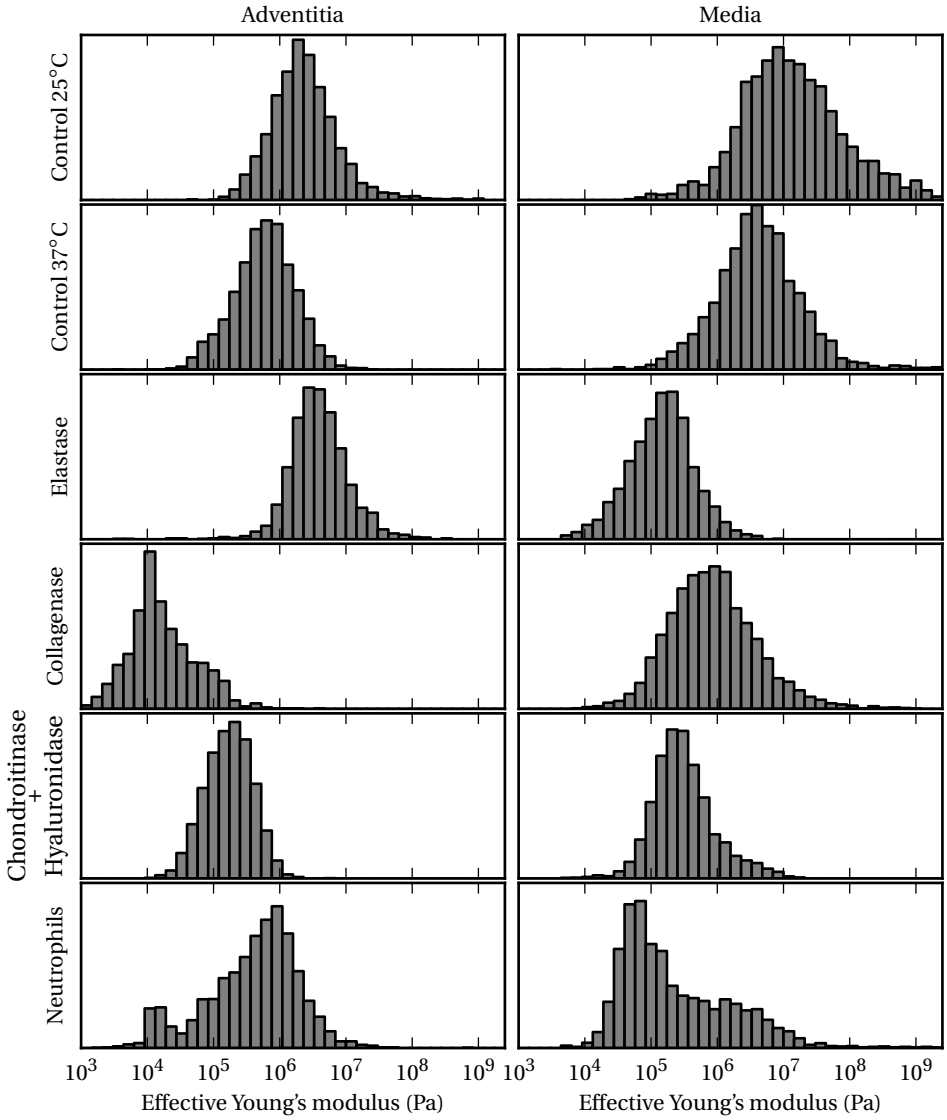

Figure 5.3:
Histograms showing the stiffness distribution of the porcine aortic wall after various proteolytic treatments. The plot shows a clear decrease in effective Young's modulus in certain conditions. For every condition at least 2000 indentations on different locations have been performed. All measurements have been performed at 37 °C, except for one control and the elastase treatment which have been performed at 25 °C. A maximum indentation force of 20 nN was used.

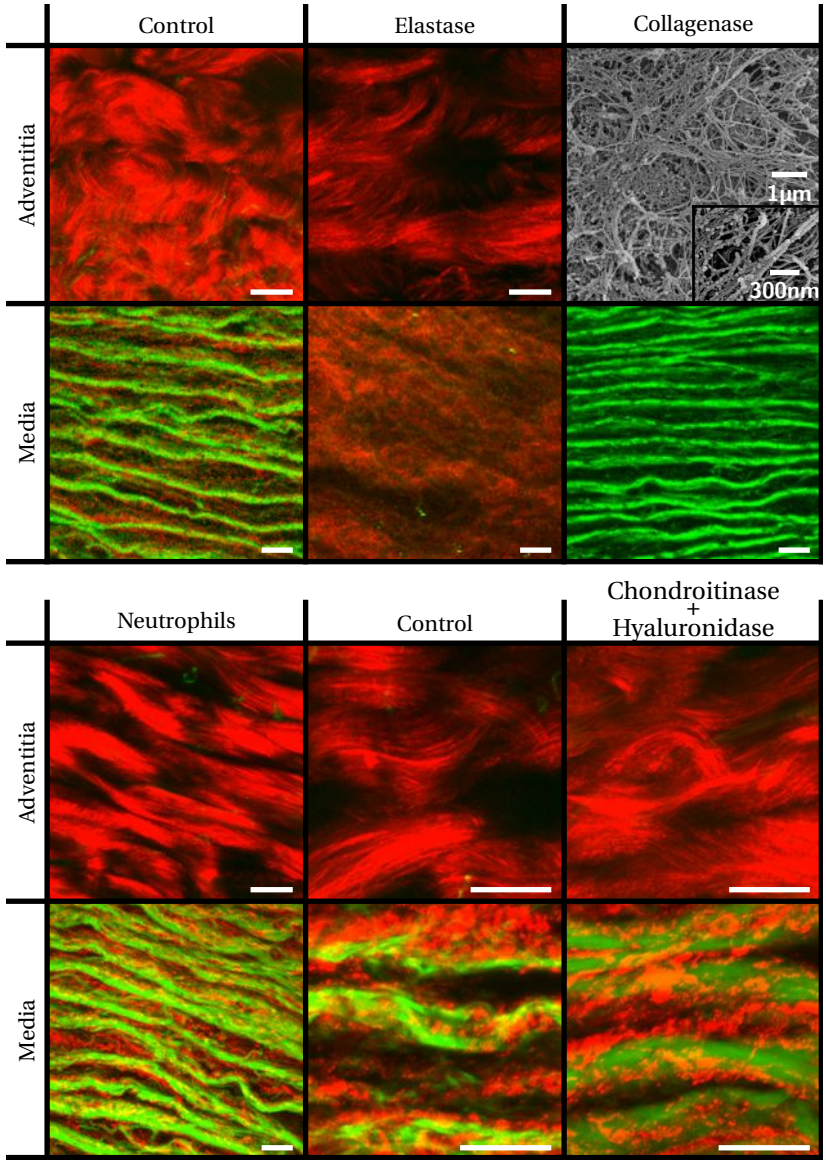

Figure 5.4:
Two photon microscopy images of the porcine aortic wall after various proteolytic treatments. Scale bars are 20µm. The images show a clear removal of the autofluorescence signal corresponding to elastin (green) or the SHG signal corresponding to collagen (red) fibers in certain conditions.
The adventitia did not give any signal after the collagenase treatment. Instead SEM images, at a higher magnification, of the remaining tissue are shown. Please note that, because the effects of chondroitinase and hyaluronidase treatments are expected to take place on a smaller length scale compared to the other treatments, the images of this treatment are made at a higher magnification. The sample used for the two photon experiments with the neutrophils had a four times as high penicillin-streptomycin concentration as is listed in table 5.1.

with this temperature has also been made. The observed small decrease in stiffness between the control sample left overnight at an incubation temperature of 37 °C, compared to an incubation temperature of 25 °C, is much smaller than the changes made by the proteolytic treatments.

Colagenase treatment weakens both layers. The weakening of the adventitia, an approximate 45-fold decrease in stiffness, is stronger than in the media, where the stiffness decreases by approximately a factor 3. Although two-photon imaging shows no collagen and elastin present in the digested adventitia, the AFM still feels a coherent network. SEM imaging confirms the existence of a remaining coherent network. The remaining structures have a large similarity with the structure of proteoglycans, which have been reported to be present in both layers of the aortic wall.[19, 20]

Removal of the proteoglycans by a mixture of Chondroitinase ABC and Hyaluronidase showed reduced stiffness of both media and adventitia. This decrease is modest compared to the collagenase treatment of the adventitia or the elastase treatment of the media, but it is still quite significant, considering that the two-photon images do not reveal any significant change in the network structure.

Different studies suggest that neutrophils are associated with degradation of the extracellular matrix. The large number of different enzymes, contained in neutrophils,[23] have been shown to be capable of removing proteoglycans,[24–26] collagen[27] and elastin[28] from the ECM. The visually unaltered collagen and elastin structure in the multi-photon images suggest that the concentration of collagen and elastin degrading enzymes is too low to significantly alter those networks. The AFM nano-indentation measurements, however, do show a weakening similar to the weakening of the tissue when the combination of Chondroitinase ABC and Hyaluronidase is applied. This could imply that there is a sufficient concentration of proteoglycan degrading enzymes in the neutrophil extract to alter these components of the ECM. The larger spread in measured stiffnesses could be the result of ECM degrading enzymes that do locally damage the collagen and elastin network.

A close look at the individual nano-indentation curves, depicted in fig. 5.5, shows additional information concerning the mechanical interaction on the fiber level. While untreated or unaltered tissue shows a steep increase of the force upon indentation, we find that when a main component of the extra cellular matrix is removed, eg. collagen from the adventitia, the elasticity of the tissue not only decreases, but also many drops in force are observed, which we interpret as breaking events (denoted by asterixes in fig. 5.5b–d).

A large number of indentation curves of the neutrophil treated adventitia show a piecewise linear increasing force upon indentation, indicating that the AFM tip pushes on an individual fiber instead of on a well connected network. The

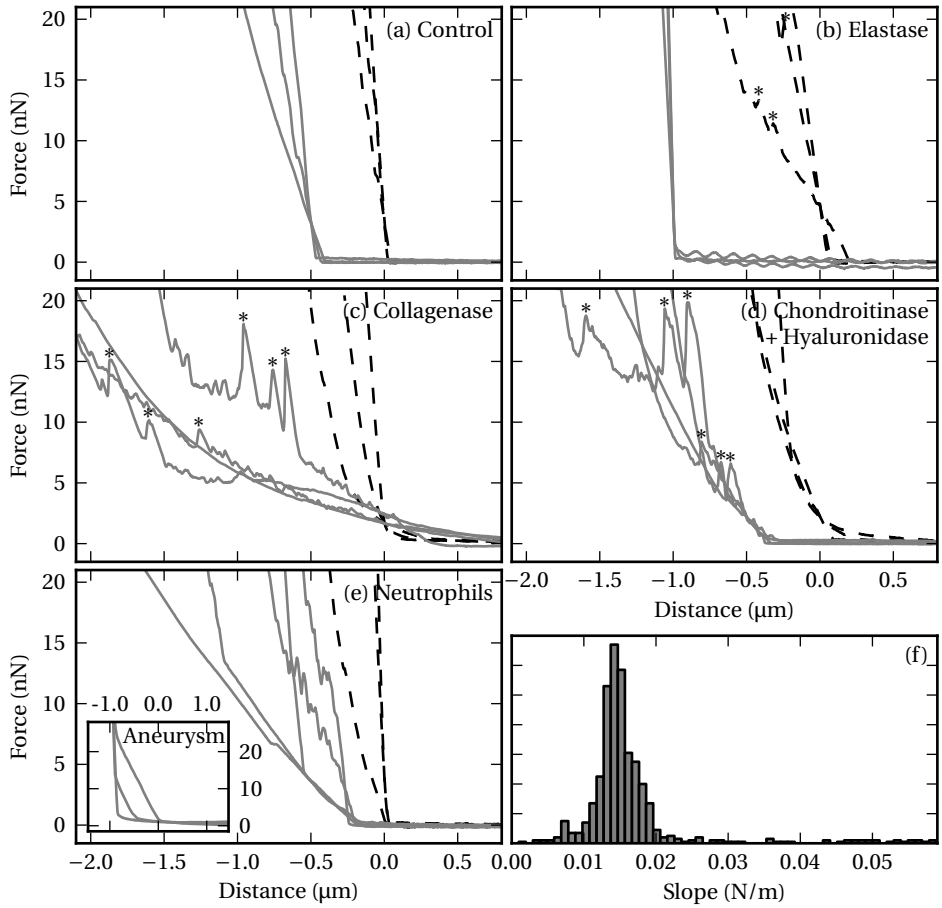

Figure 5.5:
(a-e) Representative nano-indentation curves after various proteolytic treatments of the adventitia (continous lines) and the media (striped lines) of the porcine aorta. Some of the breakage events are marked with a *. These curves gives a clear signal of the mechanical interaction on the fiber level. Untreated or unaltered tissue shows a steep increase of the force upon indentation. When a main component of the extra cellular matrix is removed, the elasticity of the tissue not only decreases, but also many drops in force are observed.
The inset of e) shows three representative nano-indentation curves measured on an aneurismatic aorta of a human donor (data taken from chapter 4[29]). In (e) a similar piecewise linear increase is measured on an adventitia treated with the contents of activated neutrophils.
(f) Histogram of slopes of the first increasing part of the nano-indentation curves of a neutrophil treated adventitia. The distribution shows a clear peak around 0.014 N/m. The data of this graph is taken from one of the two locations on which the piece-wise linear increasing force was measured.

piece-wise linear curves of the neutrophil treated adventitia show a peak in the stiffness distribution, at 10^4 and at 10^5 Pa, depending on the stiffness of the AFM cantilever. This shows that the Hertz model does not apply for these curves because the slope of the force-distance curve is a measure for the ratio of the stiffness of the cantilever and the fiber on which it pushes and not for the Young's modulus of the sample.

A complicating factor of the neutrophil data arises from the fact that its action is consistently non-uniform. Only two out of five different 113µm × 113µm grids (from two independent experiments) on which the nano-indentation measurements were performed, showed the piecewise linear increasing force, while the other three grids did not, revealing an inhomogeneity of the tissue on larger length scales. However, some of the indentations on these three grids, did show a piece-wise linear decreasing force on the retracting part only of the indentation. The control measurements, taken on four different locations from two independent measurements, did not show any non-uniformity between the measurement locations. Alcian blue staining for proteoglycans, fig. 5.6, confirmed the emergence of inhomogeneity on a length scale larger than the scan-size of the AFM . At present we cannot attribute the non-uniformity to a specific blocking agent simply because we do not know which of the many components of the neutrophil extract is responsible for the observed change.

The sharp distribution of slopes of the first linear part after indentation, figure 5.5f, shows that the different fibers have the same stiffness. Previous studies on aneurysmatic tissue, chapter 4, showed a similar piecewise linear force increase upon indentation,[29] which is shown in the inset of fig. 5.5e. Aneurysms, a local dilatation of the arterial wall, are characterized by an inflammatory vessel wall, containing a highly elevated number of neutrophils.[30–32] The fact that an overnight incubation with the contents of activated neutrophils is enough to mimic the change in response from a healthy to an aneurysmatic tissue both in the stiffness and in the shape of the indentation curve, suggests that neutrophils may be responsible for the change in the mechanical properties of aneurysmatic aortic tissue of humans on the nanometer scale.

These measurements show how enzymes, secreted by cells, alter the mechanical properties of their surroundings. Other studies have shown that mechanical strain affects the ECM and enzyme production of cells. Vascular smooth muscle cells, for example, not only produce more fibronectin, collagen[33] and proteoglycans[34] when strained, the expression of the collagen degrading matrix metalloproteinase 2 is also increased.[33, 35] These effects, which strongly depend on the specific interactions between the cells and the ECM,[36] have also been shown in skin tissue,[37] synovial joints[38] and bone.[39, 40]

5.5 Conclusion

This study shows how the contribution of the individual components of the ECM to its mechanical properties is different for the adventitial and medial layers of the aorta. Although the removal of collagen, a key element of the ECM, is capable of reducing the local stiffness up to 50 times, the remaining tissue still forms a coherent network. The revealed micro-architecture and stiffness of the individual network components can be used as a basis for further theoretical studies, to better understand the interplay between fiber mechanics and the network organization.

Furthermore, we believe the significance of this study is demonstrated by the effect of the contents of activated neutrophils on the aortic wall. An overnight incubation with the contents of activated neutrophils is able to reproduce the change of local mechanical properties observed in aneurysms. Although this does not explain the previously observed remodeling of the collagen fibers on a larger length scale,[29] it is very well possible that the local change in mechanical properties, caused by the neutrophils, might trigger other cells to weave the new collagen fibers to repair the tissue in a different, less ordered, way. Further studies are needed to elucidate which components of the extra cellular matrix are altered by enzymes of the neutrophils and how this gives rise to a distinct response upon indentation.

We believe that this new way of studying the mechanical properties of the extra cellular matrix is not only valuable for physicists to get a better understanding of the mechanical properties of biopolymers, it will also help biomedical researchers to study processes like wound healing, atherosclerotic plaque development and cervix ripening. These are all processes in which the interaction between cells and their environment results in a remodeling of the extra cellular matrix.

5.6 Supporting material

In order to see whether proteoglycans could be at the origin for the observed non-uniformity in the adventitia after the treatment with the neutrophil extract, we stained samples, after incubation with either PBS or the neutrophil extract, for proteoglycans using alcian blue, fig. 5.6.

The alcian blue stained sample of the neutrophil treated tissue reveals bands of more intense staining in the adventitia that do not appear in the controls. The width of those bands, which exceed 100µm, are comparable to the area which is examined within one AFM measurement, which could explain why we do not see the piece-wise linear force curves in all measurements. We do not

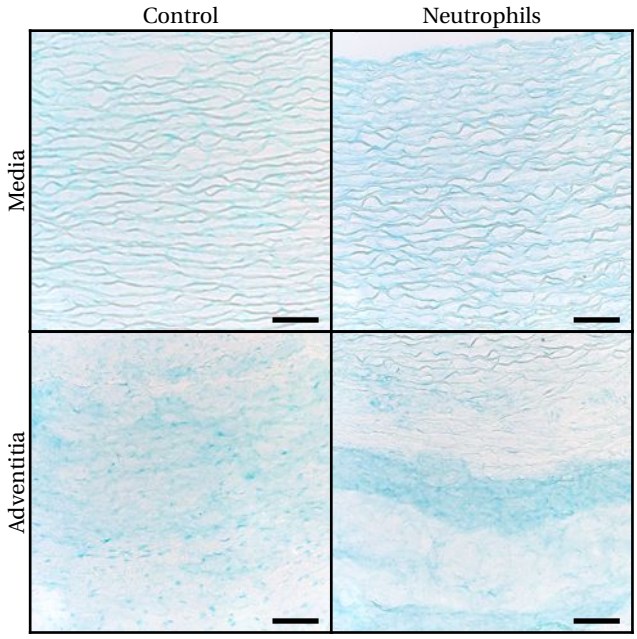

Figure 5.6:
Alcian blue staining of the media and adventitia of a control and neutrophil treated sample shows the presence of proteoglycans in both layers. The adventitia of the neutrophil extract treated sample shows bands with an increased staining.
Scale bars are 100µm.

know the mechanism that produces this non-homogeniety, but neutrophils are known to affect proteoglycans.[24–26] The increased staining could be caused by the cutting of large proteoglycans into smaller units, but could also be the result of unmasking: the enzymes removed some components from the ECM allowing more proteoglycans to be stained.

Methods

The samples have been prepared and treated with the enzymes as described section 5.3. After the overnight incubation with the enzymes, the buffer with the enzymes has been removed from the sample and the samples have been dried in air for 2 hours. Afterwards the samples are fixated by putting them 10 minutes in acetone and are stained in Alcian blue solution (Merck, Darmstadt, Germany) for 8 minutes. Subsequently they are rinsed three times by dipping them for 2 minutes in water. Afterwards they are dried in air and covered.

5.7 Acknowledgements

We thank T. Cerami for stimulating discussions, A. van der Laan and H. Tanke for their help and use of the two photon microscope, R. van Dijk for the movat stained arterial wall, J. Onderwater and A. Koster for their help and use of the SEM and P. Nibbering for the preparation of the contents of the activated neutrophils. This project is financially supported by a Netherlands SmartMix grant and the NIMIC partner organizations (www.nimic-project.com) through NIMIC, a public-private program.

5.8 References

[1] D. A. Vader, A. Kabla, D. A. Weitz, and L. Mahadevan. Strain-induced alignment in collagen gels. *arXiv*, cond-mat.soft:e5902, 2009.

[2] F. Backouche, L. Haviv, D. Groswasser, and A. Bernheim-Groswasser. Active gels: dynamics of patterning and self-organization. *Phys. Biol*, 3:264, 2006.

[3] I. K. Piechocka, A. S. G. van Oosten, R. G. M. Breuls, and G. H. Koenderink. Rheology of heterotypic collagen networks. *Biomacromolecules*, 12:2797, 2011.

[4] C. Storm, et al. Nonlinear elasticity in biological gels. *Nature*, 435:191, 2005.

[5] J. S. Bartholomew and J. C. Anderson. Investigation of relationships between collagens, elastin and proteoglycans in bovine thoracic aorta by immunofluorescence techniques. *Histochem. J.*, 15:1177, 1983.

[6] H. M. Walker-Caprioglio, et al. Organization of rat mesenteric artery after removal of cells of extracellular matrix components. *Cell Tissue Res.*, 264:63, 1991.

[7] M. R. Roach and A. C. Burton. The reason for the shape of the distensibility curves of arteries. *Can. J. Biochem. Physiol.*, 35:681, 1957.

[8] P. B. Dobrin and T. R. Canfield. Elastase, Collagenase, and the Biaxial Elastic Properties of Dog Carotid-Artery. *Am. J. Physiol.*, 247:H124, 1984.

[9] P. B. Dobrin, W. H. Baker, and W. C. Gley. Elastolytic and collagenolytic studies of arteries. Implications for the mechanical properties of aneurysms. *Arch. surg.*, 119:405, 1984.

[10] A. S. Hoffman and J. Park. Sequential Enzymolysis of Human Aorta and Resultant Stress-Strain Behavior. *Biomater. Artif. Cell*, 5:121, 1977.

[11] J. A. Kratzberg, P. J. Walker, E. Rikkers, and M. L. Raghavan. The effect of proteolytic treatment on plastic deformation of porcine aortic tissue. *J. Med. Behav. Biomed. Mater.*, 2:65, 2009.

[12] M. J. A. van der Plas, et al. Maggot excretions/secretions inhibit multiple neutrophil pro-inflammatory responses. *Microbes Infect.*, 9:507, 2007.

[13] A. Zoumi, X. Lu, G. Kassab, and B. Tromberg. Imaging coronary artery microstructure using second-harmonic and two-photon fluorescence microscopy. *Biophys. J.*, 87:2778, 2004.

[14] E. A-Hassan, et al. Relative microelastic mapping of living cells by atomic force microscopy. *Biophys. J.*, 74:1564, 1998.

[15] I. N. Sneddon. The relation between load and penetration in the axisymmetric Boussinesq problem for a punch of arbitrary profile. *Int. J. Eng. Sci.*, 1965.

[16] H. J. Butt and M. Jaschke. Calculation of Thermal Noise in Atomic-Force Microscopy. *Nanotech.*, 6:1, 1995.

[17] W. M. Lai, J. S. Hou, and V. C. Mow. A Triphasic Theory for the Swelling and Deformation Behaviors of Articular Cartilage. *J. Biomech. Eng.*, 113:245, 1991.

[18] A. I. Maroudas. Balance between swelling pressure and collagen tension in normal and degenerate cartilage. *Nature*, 260:808, 1976.

[19] T. N. Wight. Vessel proteoglycans and thrombogenesis. *PNAS*, 5:1, 1980.

[20] L. Y. Yao, et al. Identification of the proteoglycan versican in aorta and smooth muscle cells by DNA sequence analysis, in situ hybridization and immunohistochemistry. *Matrix Biol.*, 14:213, 1994.

[21] X. Guo, Y. Lanir, and G. S. Kassab. Effect of osmolarity on the zero-stress state and mechanical properties of aorta. *Am. J. Physiol. Heart Circ. Physiol.*, 293:H2328, 2007.

[22] E. U. Azeloglu, et al. Heterogeneous transmural proteoglycan distribution provides a mechanism for regulating residual stresses in the aorta. *Am. J. Physiol. Heart Circ. Physiol.*, 294:H1197, 2008.

[23] M. Faurschou and N. Borregaard. Neutrophil granules and secretory vesicles in inflammation. *Microbes Infect.*, 5:1317, 2003.

[24] Y. Matzner, et al. Degradation of heparan sulfate in the subendothelial extracellular matrix by a readily released heparanase from human neutrophils. Possible role in invasion through basement membranes. *J. Clin. Invest.*, 76:1306, 1985.

[25] D. Shum and S. Chan. Neutrophil-Mediated Degradation of Lung Proteoglycans. Stimulation by Tumor Necrosis Factor-alpha in Sputum of Patients with Bronchiectasis. *Am. J. Med. Sci.*, 2000.

[26] S. E. McGowan. Mechanisms of extracellular matrix proteoglycan degradation by human neutrophils. *Am. J. Respir. Cell Mol. Biol.*, 2:271, 1990.

[27] K. A. Hasty, et al. Human Neutrophil Collagenase - a Distinct Gene-Product with Homology to Other Matrix Metalloproteinases. *J. Biol. Chem.*, 265:11421, 1990.

[28] J. C. Powers, et al. Specificity of Porcine Pancreatic Elastase, Human Leukocyte Elastase and Cathepsin-G-Inhibition with Peptide Chloromethyl Ketones. *Biochim. Biophys. Acta*, 485:156, 1977.

[29] J. H. N. Lindeman, et al. Distinct defects in collagen microarchitecture underlie vessel-wall failure in advanced abdominal aneurysms and aneurysms in Marfan syndrome. *PNAS*, 107:862, 2010.

[30] J. R. Cohen, et al. Role of the neutrophil in abdominal aortic aneurysm development. *Cardiovasc. Surg.*, 1:373, 1993.

[31] M. B. Pagano, et al. Complement-dependent neutrophil recruitment is critical for the development of elastase-induced abdominal aortic aneurysm. *Circulation*, 119:1805, 2009.

[32] J. Eliason, et al. Neutrophil depletion inhibits experimental abdominal aortic aneurysm formation. *Circulation*, 112:232, 2005.

[33] C. O'Callaghan and B. Williams. Mechanical strain-induced extracellular matrix production by human vascular smooth muscle cells - Role of TGF-beta(1). *Hypertension*, 36:319, 2000.

[34] R. Lee, et al. Mechanical strain induces specific changes in the synthesis and organization of proteoglycans by vascular smooth muscle cells. *J. Biol. Chem.*, 276:13847, 2001.

[35] D. Seliktar, R. M. Nerem, and Z. S. Galis. Mechanical Strain-Stimulated Remodeling of Tissue-Engineered Blood Vessel Constructs. *Tissue Eng.*, 9:657, 2003.

[36] E. Wilson, K. Sudhir, and H. Ives. Mechanical Strain of Rat Vascular Smooth-Muscle Cells Is Sensed by Specific Extracellular Matrix/Integrin Interactions. *J. Clin. Invest.*, 96:2364, 1995.

[37] N. Bhadal, et al. The effect of mechanical strain on protease production by keratinocytes. *Brit. J. Dermatol.*, 158:396, 2007.

[38] G. Dowthwaite, et al. The effect of mechanical strain on hyaluronan metabolism in embryonic fibrocartilage cells. *Matrix Biol.*, 18:523, 1999.

[39] A. Kadow-Romacker, et al. Effect of Mechanical Stimulation on Osteoblast- and Osteoclast-Like Cells in vitro. *Cells Tissues Organs*, 190:61, 2009.

[40] M. Buckley, A. Banes, and R. Jordan. The effects of mechanical strain on osteoblasts in vitro. *J. Oral Maxil. Surg.*, 48:276, 1990.